

# Study of polycrystalline sintered compacts of diamond

BHANU PRATAP SINGH

National Physical Laboratory, New Delhi 110 012, India

Study of polycrystalline sintered compacts of diamond has been made using powder X-ray diffraction, scanning electron microscopy (SEM) and energy-dispersive X-ray analysis (EDX). Various crystalline phases formed at high temperature and high pressure, microstructure, particle-size distribution of diamond and binder and concentration of different elements in the sintered diamond compacts were determined.

## 1. Introduction

Polycrystalline sintered compacts of diamond are extensively used as cutting tools in machining hard and abrasive materials. These compacts are synthesized at high temperature and high pressure with or without metal binders. Stromberg and Stephens [1], Hall [2] and Suzuki *et al.* [3] have reported sintering of diamond compacts without the use of a binder. Katzman and Libby [4], Wentorf and Rocco [5], Notsu *et al.* [6] and Akaishi *et al.* [7] have reported the high-pressure sintering of diamond using cobalt as the binder. The sintering conditions and the role of cobalt in the sintering process have been discussed by these scientists. The sintered compacts were also characterized for crystalline phases, microstructure and hardness. Cobalt (cubic) was the only other crystalline phase detected in the sintered diamond apart from diamond [4, 6, 7]. However, Notsu *et al.* [6] reported the presence of some weak X-ray diffraction peaks which they ascribed to be probably due to the formation of a eutectic mixture of cobalt and graphite. No details of binders/impurities other than cobalt in the sintered compacts of diamond have been reported. Results of a detailed analysis of particle-size distribution of diamond and binder particles in the diamond compacts have not been reported. However, the particle-size range of starting diamond powders was reported by most of the earlier investigators.

In the present investigation a detailed compositional analysis and particle-size distribution of diamond and binder particles in the polycrystalline sintered compacts of diamond were carried out. Powder X-ray diffraction was used to study the various crystalline phases that are formed at high temperature and high pressure. Microstructure and particle size distribution of diamond and binder particles were evaluated using scanning electron microscopy (SEM). Energy-dispersive X-ray (EDX) analysis was employed for the determination of concentration of different elements present. Results of these investigations are reported in this paper.

## 2. Experimental details

### 2.1. Samples

Two types of diamond compacts, Types A and B,

obtained from different sources have been used in the present investigation.

### 2.2. Techniques

Powder X-ray diffraction was used to study the different crystalline phases that are formed at high temperature and high pressure in the sintered diamond compacts. The diffractograms were recorded in reflection geometry using  $\text{CuK}\alpha$  as the exploring beam.

Scanning electron microscopy (SEM) was used to study microstructure and particle-size distribution of diamond and binder particles in diamond compacts. A ISI-Super-III SEM was used for this purpose. All the micrographs were recorded in the secondary-electron-emission mode with  $0^\circ$  tilt.

Elemental analysis in sintered diamond compacts was carried out by energy-dispersive X-ray analysis. An electron beam of 30 kV and  $0^\circ$  tilt was used to excite the characteristic X-ray spectra of the constituent elements. The distance between specimen and detector was 30 mm. A working distance of 16 mm was used. The spot size was kept constant at its maximum in order to increase the emitted X-ray photons. A counting interval of 200 sec was used for counting the emitted X-ray photons from the constituent elements in the diamond compacts. These experimental parameters were fixed constant for the unknown specimen as well as for the standard reference elements involved. The X-ray spectra were analysed with a Tracor Northern TN2700 spectrum analyser.

## 3. Results and discussion

### 3.1. X-ray characterization

Fig. 1 shows a typical powder X-ray diffraction pattern obtained for diamond compacts of Type A. The diffraction maximum observed at  $2\theta = 43.9^\circ$  ( $d = 0.206$  nm) is due to superposition of (111) reflections of diamond and  $\beta$ -cobalt (cubic). Here  $\theta$  is the Bragg angle and  $d$ , the interplanar spacing. As the  $d$ -values of diamond (0.206 nm) and  $\beta$ -cobalt (0.20467 nm) for the (111) reflection are very close to each other, these reflections are not resolved in the present experimental conditions ( $\beta$ -filtered  $\text{CuK}\alpha$ -radiation with a divergence of  $1^\circ$ ). The diffraction

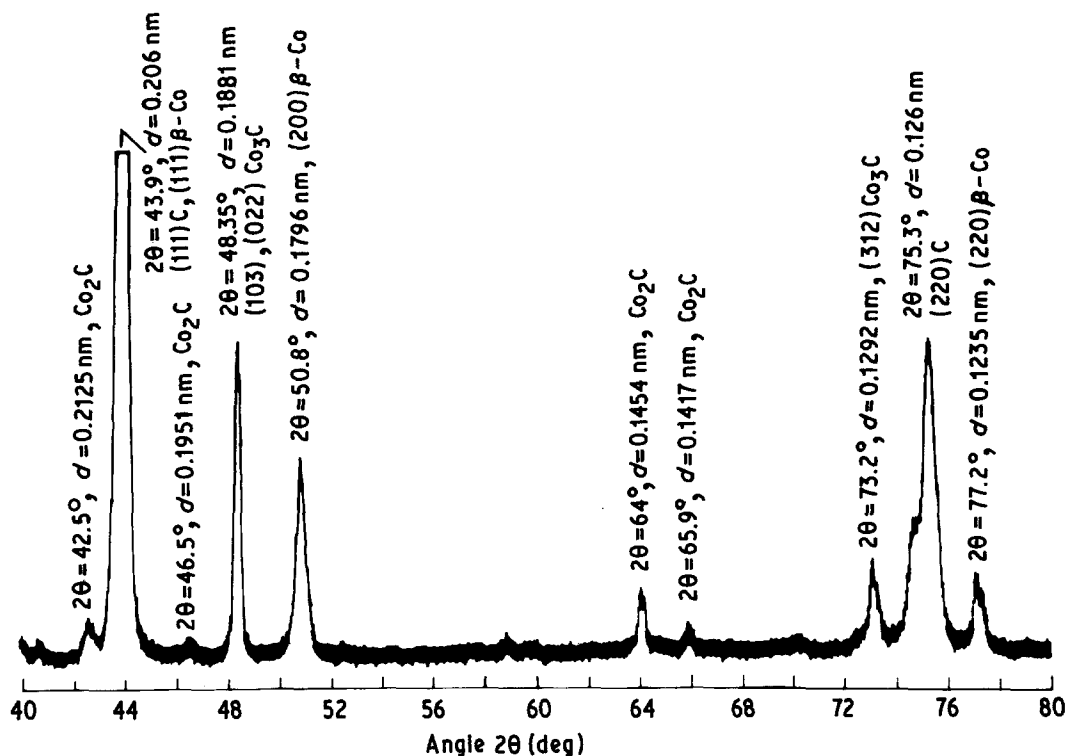


Figure 1 Powder X-ray diffraction pattern of diamond compact of Type A using  $\text{CuK}\alpha$  as the exploring beam.

maxima observed at  $2\theta = 75.3^\circ$  ( $d = 0.126 \text{ nm}$ ) and  $77.2^\circ$  ( $d = 0.1235 \text{ nm}$ ) are due to (220) reflections of diamond and  $\beta$ -cobalt, respectively. A diffraction maximum observed at  $2\theta = 50.8^\circ$  ( $d = 0.1796 \text{ nm}$ ) is due to the (200) reflection of  $\beta$ -cobalt. No reflections due to  $\alpha$ -cobalt (hexagonal) are observed.

It is seen in Fig. 1 that there are many sharp and intense X-ray diffraction lines which do not correspond to either diamond or  $\beta$ -cobalt. These diffraction maxima are observed at  $2\theta = 42.5^\circ$  ( $d = 0.2125 \text{ nm}$ ),  $48.35^\circ$  ( $d = 0.1881 \text{ nm}$ ),  $64.0^\circ$  ( $d = 0.1454 \text{ nm}$ ),  $65.9^\circ$  ( $d = 0.1417 \text{ nm}$ ) and  $73.2^\circ$  ( $d = 0.1292 \text{ nm}$ ). These are due to the formation of a eutectic mixture of cobalt and carbon which might have precipitated as carbides of cobalt during the later stages of sintering process. It is observed that both  $\text{Co}_2\text{C}$  and  $\text{Co}_3\text{C}$  are present in specimens of Type A diamond compact. The corresponding values of  $2\theta$  together with their interplanar spacings for observed reflections of the two phases of cobalt carbide have been marked in Fig. 1. The ASTM cards used were 5-0704 ( $\text{Co}_2\text{C}$ ) and 26-450 ( $\text{Co}_3\text{C}$ ). It is interesting to note that the crystal structure and lattice parameters of  $\text{Co}_2\text{C}$  are still unknown. Notsu *et al.* [6] also observed some weak diffraction lines in one of the specimens of diamond compact, in addition to cobalt and diamond, which they thought to be probably due to the formation of a eutectic mixture of cobalt and graphite.

Fig. 2 shows a typical powder X-ray diffraction pattern obtained for diamond compacts of Type B using  $\text{CuK}\alpha$  as the exploring beam. The different diffraction lines observed have been marked in Fig. 2 along with their values of  $2\theta$  and  $d$ . The general features of the powder diffraction pattern observed for this specimen are similar to those obtained for diamond compacts of Type A. In this case also, the

crystalline phases observed are: diamond,  $\beta$ -cobalt and carbides of cobalt.

### 3.2. Microstructure and particle-size analysis

Figs 3a and b show typical SEMs obtained for diamond compacts of Types A and B, respectively. Black regions represent diamond grains and white regions represent cobalt particles. It can be seen that in both types of specimen, diamond grains are uniformly distributed in the cobalt matrix. The diamond grains are well bonded against each other through fusion of cobalt particles in the intergranular spaces. In some regions diamond particles appear to be fused together in the form of clusters. Clustering of cobalt particles is also observed. There are regions where the boundaries between diamond grains are not clearly outlined. This is because of partial dissolution of diamond surface by melted cobalt. Therefore, in such a situation slight grain growth is unavoidable because the dissolved diamond would reprecipitate on some other diamond grains.

Particle-size distributions of diamond and binder grains were determined from SEMs. Because the signal to background ratio for diamond grains was poor it was not possible to carry out image analysis using an image analyser. Therefore, the particle-size distribution of diamond and binder particles was obtained manually from the magnified SEMs. Several SEMs of diamond compacts of both the types were recorded for this purpose. In determining the particle sizes of diamond and binder particles the concept of particle size as adopted by Federation Europeene des Fabricants de Produits Abrasifs (FEPA) was used. This concept is as follows: "the diameter of the circle which completely encloses the particle is said to define the particle size".

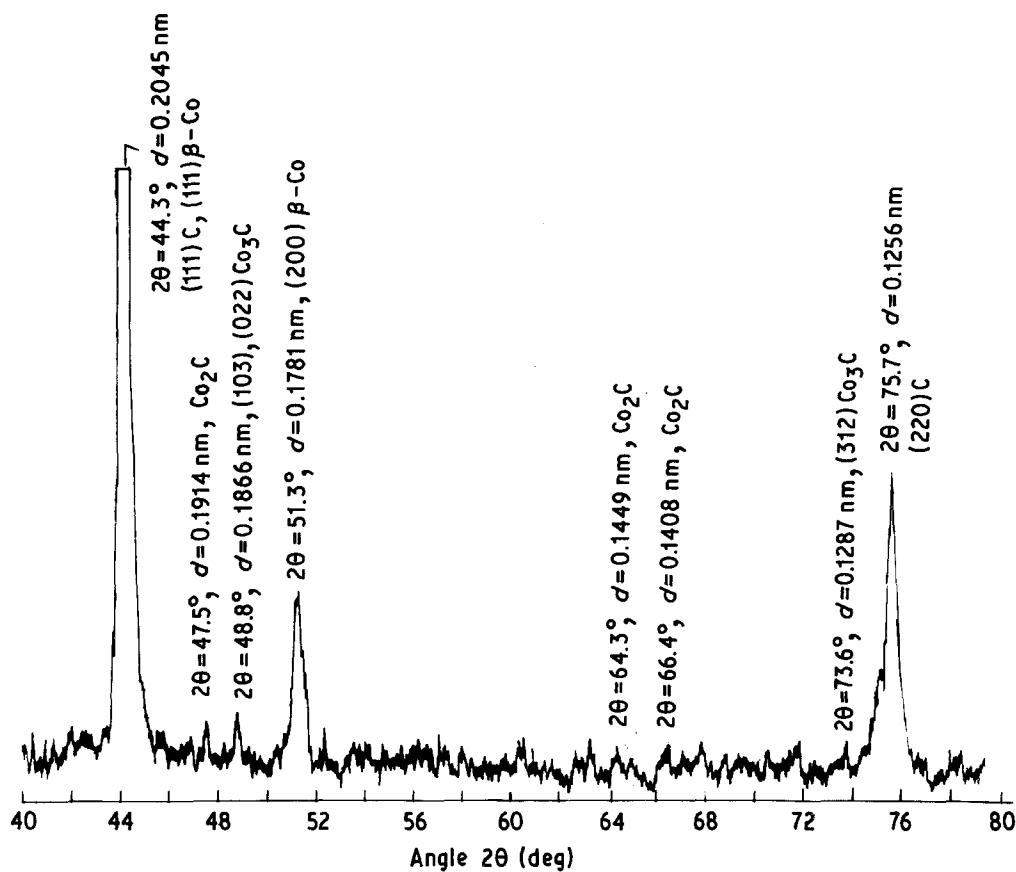


Figure 2 Powder X-ray diffraction pattern of diamond compact of Type B using CuK $\alpha$  as the exploring beam.

Table I shows the results of particle-size distribution analysis made on diamond compacts of Types A and B. This table represents the percentage distribution of diamond and binder particles having a particular particle size in diamond compacts. For a diamond compact of Type A, the particle size of diamond particles ranges from 2 to 6  $\mu\text{m}$ , with about 50% of the diamond particles having a particle size of 3  $\mu\text{m}$ . The particle size of binder lies between 0 and 2  $\mu\text{m}$ , with about 60% of binder particles having particle sizes less than 1  $\mu\text{m}$ . For diamond compacts of Type B, the particle size of diamond particles ranges from 10 to 30  $\mu\text{m}$ , with 45% of the diamond particles having a particle size of 15  $\mu\text{m}$ . The particle size of

binder particles ranges from 2 to 6  $\mu\text{m}$ . Furthermore, about 64% of the binder particles have their particle sizes between 3 and 4  $\mu\text{m}$ .

### 3.3. Elemental analysis

Elemental analysis was carried out for the diamond compacts of Types A and B using the EDX technique. The experimental conditions for obtaining characteristic X-ray spectra of the constituent elements in the unknown specimen and the standard reference elements involved were fixed constant. It should be mentioned that the determined values of weight percentages of the elements in the diamond compacts represent absolute values. These values were deter-

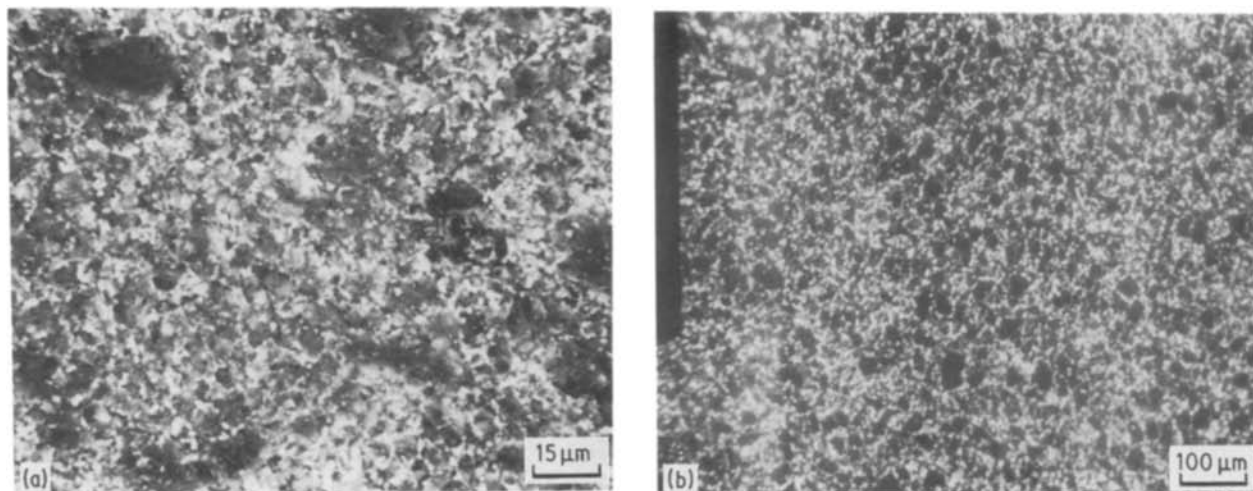


Figure 3 Typical scanning electron micrographs for diamond compacts of (a) Type A, and (b) Type B.

TABLE I Particle-size distribution of diamond and binder in diamond compacts

Diamond compact type	Diamond particles		Binder particles	
	% Particles	Particle size ( $\mu\text{m}$ )	% Particles	Particle size ( $\mu\text{m}$ )
A	10.0	2.1	61.4	0.7
	33.3	2.8	35.6	1.4
	26.6	3.5	4.0	2.1
	13.3	4.2		
	10.0	4.9		
	3.3	5.6		
	3.5	6.3		
B	8.0	10.0	23.5	2.0
	14.4	12.0	44.0	3.0
	45.0	15.0	20.5	4.0
	12.2	18.0	6.0	5.0
	10.4	20.0	6.0	6.0
	6.0	25.0		
	4.0	30.0		

mined by comparing the X-ray counts for 200 sec emitted by the elements in the given compact to the corresponding values obtained for pure elements involved. The following weight % of elements in the diamond compacts of Types A and B were determined:

Type A: Co(16.0 wt %), Fe(1.0 wt %), Ni(0.5 wt %), Al(0.1 wt %).

Type B: Co(15.0 wt %), Fe(0.8 wt %), Cr(0.1 wt %), Al(0.06 wt %).

#### 4. Conclusion

The crystalline phases that were detected in the diamond compacts of Types A and B were practically the same, namely diamond,  $\beta$ -cobalt and cobalt carbides.

Particle-size distribution analysis of diamond and binder in the diamond compacts of Types A and B showed the following size distributions:

##### Type A

diamond particles: 2 to 6  $\mu\text{m}$  with peak value around 3  $\mu\text{m}$ .

binder particles: 0 to 2  $\mu\text{m}$  with a peak value of 1  $\mu\text{m}$ .

##### Type B

diamond particles: 10 to 30  $\mu\text{m}$  with a peak value around 15  $\mu\text{m}$ .

binder particles: 2 to 6  $\mu\text{m}$  with a peak value 3 to 4  $\mu\text{m}$ .

Quantitative elemental analysis made on diamond compacts of Types A and B using the EDX technique yielded the following weight % of elements present:

Type A: Co(16.0 wt %), Fe(1.0 wt %), Ni(0.5 wt %), Al(0.1 wt %).

Type B: Co(15.0 wt %), Fe(0.8 wt %), Cr(0.1 wt %), Al(0.06 wt %).

#### Acknowledgements

The author is grateful to the Director, National Physical Laboratory, New Delhi for his interest in this work. The financial support provided by UNDP is gratefully acknowledged. The author thanks Dr B. K. Agarwala for his interest in this work and for providing the specimens used, Dr M. M. Bindal for his cooperation, Dr T. Negas for providing facilities for EDX analysis and Dr E. Steel for providing pure elements used in EDX analysis.

#### References

1. H. D. STROMBERG and D. R. STEPHENS, *Ceram. Bull.* **49** (1970) 1030.
2. H. T. HALL, *Science* **169** (1970) 868.
3. N. SUZUKI, A. NAKAUE and O. OKUMA, *J. Jpn High Press. Sci.* **11** (1974) 301.
4. H. KATZMAN and W. F. LIBBY, *Science* **172** (1971) 1132.
5. R. H. WENTORF JR and W. A. ROCCO, US Patent 3745 623 (1973).
6. Y. NOTSU, T. NAKAJIMA and N. KAWAI, *Mater. Res. Bull.* **12** (1977) 1079.
7. M. AKAISHI, H. KANDA, Y. SATO, N. SETAKA, T. OHSAWA and O. FUKUNAGA, *J. Mater. Sci.* **17** (1982) 193.

Received 22 July

and accepted 16 October 1986